

# Experimental and Modeling Study on Gas Hydrate Formation Kinetics of (Methane + Ethylene + Tetrahydrofuran + H<sub>2</sub>O)<sup>†</sup>

Qing-Lan Ma,\* Guang-Jin Chen, and Ling-Wei Zhang

State Key Laboratory of Heavy Oil Processing, China University of Petroleum, Beijing 102249, PR China

The formation of gas hydrate was carried out for (methane + ethylene + tetrahydrofuran (THF) + H<sub>2</sub>O) in a batch stirred reactor. Experimental data on the number of gas moles consumed were obtained at pressures ranging from (1.4 to 4) MPa and at temperatures from (273.15 to 276.15) K. The influence of temperature and initial pressure on hydrate formation rate was studied, respectively. The kinetic model by Firoozabadi and co-workers coupled with the Chen–Guo hydrate model was used to predict the rate of gas hydrate formation for a gas mixture from pure gas data. This study could be useful for the recovery of ethylene from a gas mixture by forming clathrate hydrate in the chemical and petrochemical industry.

## Introduction

Separation of the low-boiling gas mixture is usually involved in oil and gas processing and ethylene production, for instance separation of methane from ethylene. The conventional distillation method requires deep cooling, which restricts obtaining high recovery efficiency. The new technology of separating a gas mixture by forming gas hydrate sparked more interest in clathrate hydrates. Gas hydrates, also called clathrate hydrates, are a sort of nonstoichiometric crystalline compound composed of water and gases with small-sized molecules,<sup>1</sup> such as CH<sub>4</sub>, C<sub>2</sub>H<sub>6</sub>, CO<sub>2</sub>, H<sub>2</sub>S, etc. The hydrate-based technique for separating gas mixtures is based on the difference of hydrate formation characteristics of various gas species. The study of gas hydrate formation kinetics is of significance in designing separation equipment and enhancing process rate and efficiency.

The study on hydrate formation kinetics usually includes two areas. The first area deals with the primary nucleation process. The second concerns the process of crystal growth. Gas hydrate nucleation and growth have been investigated by various experimental and modeling methods. Vysniauskas and Bishnoi<sup>2,3</sup> presented kinetic experimental studies on the hydrate growth of methane and ethane in the temperature range of (274 to 284) K in a semibatch stirred reactor. They fit their experimental data and developed a model for gas hydrate formation kinetics. Englezos et al.<sup>4,5</sup> coupled crystallization theory with the mass-transfer phenomena to describe gas hydrate formation kinetics. The Englezos et al. model uses the difference between the fugacity of the dissolved gas and the three-phase equilibrium fugacity as the driving force for particle growth. Kashchiev and Firoozabadi<sup>6,7</sup> analyzed the kinetics of the initial stage of crystallization of the one-component gas hydrate and developed a model to determine the rate of gas consumed. They use the difference between the chemical potential of a hydrate building unit in the aqueous solution and in the hydrate crystal<sup>8</sup> as the driving force. Duarte and Peters<sup>9</sup> experimentally studied the kinetics of formation and decomposition of hydrogen clathrate hydrate in THF aqueous solution for the first time. Experimental

data are valuable to the applicability of hydrogen clathrate hydrates as a storage medium in the transportation sector.

In this work, we measured the hydrate formation rate of (methane + ethylene + tetrahydrofuran + water) in a batch stirred reactor at three temperatures, 273.15 K, 274.15 K, and 276.15 K, and at pressures ranging from (1.4 to 4) MPa. The influence of temperature and initial pressure on the rate of gas consumption was studied. The kinetic model by Firoozabadi et al.<sup>6,7</sup> was modified and coupled with the Chen–Guo hydrate model<sup>10</sup> to describe the kinetics of gas hydrate formation. The kinetic parameters for mixtures were obtained from pure component parameters.

## Experimental Apparatus and Procedure

As we know, thermodynamic promoter THF added in water could reduce the hydrate formation pressure and induction time to accelerate the hydrate formation rate. In this work, hydrate formation kinetics for systems containing THF were studied. THF can form sII hydrate and only occupy large cavities, which implies that the mole number ratio of THF to water in hydrate should be 1:7. Therefore, the suitable concentration of THF in aqueous solution should be 0.0556 mol fraction to keep THF concentration constant during the hydrate formation procedure. In this work, the mole fraction of THF was fixed to be 0.06.

As shown in Figure 1, the apparatus consists mainly of a cylindrical high-pressure [(0 to 16) MPa] stainless steel cell with an effective volume of 256 cm<sup>3</sup>. The high-pressure cell is installed in an air-bath and equipped with a magnetic stirrer inside for accelerating the formation of hydrate. THF aqueous solution can be added or drained out through a valve at the bottom of the cell, and the (CH<sub>4</sub> + C<sub>2</sub>H<sub>4</sub>) gas mixture can be charged or vented through valves on the top of the cell. The feed gas sample is prepared in a gas cylinder. The precision of temperature and pressure measurements is within ±0.1 K and ±0.025 MPa, respectively.

A typical experiment started by washing the stainless steel cell with water and prepared THF aqueous solution three times, respectively. Air was removed from the reactor by a vacuum pump. Then, 69.82 cm<sup>3</sup> of 0.06 mol fraction THF aqueous solution was added into the cell which was installed in an air bath. The air-bath temperature was then tuned to the required

\* Corresponding author. Phone: +86 10 89733252. E-mail: maql@cup.edu.cn.

<sup>†</sup> Part of the "William A. Wakeham Festschrift".

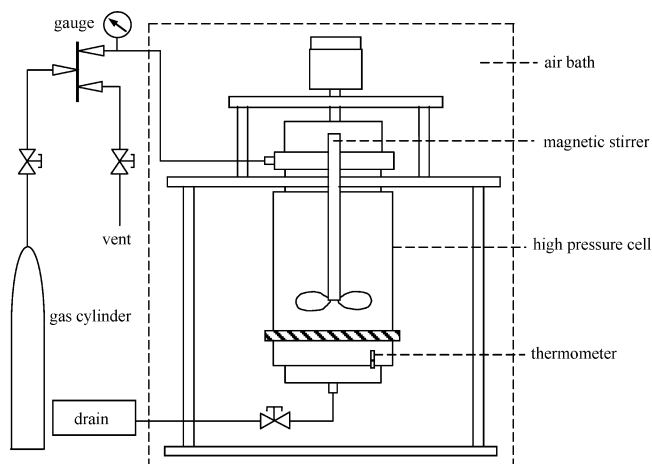


Figure 1. Schematic of the experimental apparatus.

temperature, and then the cell was charged with ( $\text{CH}_4 + \text{C}_2\text{H}_4$ ) until the required pressure was reached. The liquid phase was stirred with a magnetic stirrer, and a pressure drop began due to hydrate formation. The pressure was recorded at regular intervals until the change became slow.

### Modeling Study

**Rate of Gas Hydrate Formation.** The rate of gas hydrate formation could be expressed in terms of the gas consumption rate, which could be given as follows<sup>6,7</sup>

$$r = G^n J \quad (1)$$

$$G = K_1 \left( e^{-\frac{\Delta\mu}{RT}} - 1 \right) \quad (2)$$

$$J = K_2 e^{-\frac{\Delta\mu}{RT}} \exp\left(\frac{-A}{RT\Delta\mu^2}\right) = K_2 e^{\frac{1}{RT}\left(-\Delta\mu - \frac{A}{\Delta\mu^2}\right)} \quad (3)$$

where  $r$  is the gas consumption rate,  $\text{kmol}\cdot\text{m}^{-3}\cdot\text{min}^{-1}$ ;  $G$  is the time-independent growth rate of the separate crystallites;  $J$  denotes the stationary nucleation rate; and  $K_1$ ,  $K_2$ ,  $A$ , and  $n$  are constants. Combining  $K_1$  and  $K_2$  to one constant  $K$ , the rate of gas consumption could be expressed as

$$r = G^n J = K \left( e^{-\frac{\Delta\mu}{RT}} - 1 \right)^n e^{\frac{1}{RT}\left(-\Delta\mu - \frac{A}{\Delta\mu^2}\right)} \quad (4)$$

**Driving Force.** The difference between the chemical potential of a hydrate building unit in the aqueous solution and in the hydrate crystal<sup>8</sup> was used as the driving force in this work. The Chen–Guo two-step hydrate formation model<sup>10</sup> was used to calculate the difference of the chemical potential  $\Delta\mu$ . The two-step hydrate formation mechanism can be expressed as follows. The first step: The formation of a stoichiometric *basic hydrate* through a quasi-chemical reaction. The *basic hydrate* is defined as a complex compound formed by complete filling of the basic cavities (i.e., the large cavity) in the empty hydrate lattice with guest molecules. The second step: The adsorption of gas molecules into the empty small cavities, resulting in the nonstoichiometric property of hydrates. In this step, only small size gas molecules (e.g., Ar,  $\text{N}_2$ ,  $\text{O}_2$ ,  $\text{CH}_4$ , etc.) dissolved in water may move into the empty small cavities. On the basis of this theory,  $\Delta\mu$  is calculated as follows

$$\frac{\Delta\mu}{RT} = \lambda_1 \ln(1 - \sum_j \theta_j) + \lambda_2 \sum_i x_i^* \ln \frac{f_i^0}{f_i} \quad (5)$$

$$x_i^* = \frac{f_i}{f_i^0 [1 - \sum_j \theta_j]^{\lambda_1/\lambda_2}} \quad (6)$$

$$f_i^0 = f_{Ti}^0 \exp\left[\frac{\beta P}{T}\right] a_w^{-1/\lambda_2} \quad (7)$$

$$f_{Ti}^0 = \exp\left[\frac{-\sum_j A_{ij}\theta_j}{T}\right] \left[ A_i' \exp\left(\frac{B_i'}{T - C_i'}\right) \right] \quad (8)$$

where  $\lambda_1$  and  $\lambda_2$  stand for the numbers of small and large cavities per water molecule, respectively.  $\lambda_1 = 2/46$  and  $\lambda_2 = 6/46$  for the structure I hydrate;  $\lambda_1 = 16/136$  and  $\lambda_2 = 8/136$  for the structure II hydrate.  $x_i^*$  denotes mole fraction of component  $i$  in large cavities,  $\sum_i x_i^* = 1$ .  $a_w$  is the activity of water. The Wilson activity model<sup>11</sup> was used to calculate the activity of water and the fugacity of THF in the aqueous phase. The vapor-phase fugacity ( $f_i$ ) of component  $i$  can be calculated by EOS.  $\beta = 4.242 \text{ K}\cdot\text{MPa}^{-1}$  for structure I hydrates, and  $\beta = 10.224 \text{ K}\cdot\text{MPa}^{-1}$  for structure II hydrates.  $\theta_j$  represents the fraction of the small cavities occupied by the gas species  $j$ . On the basis of the Langmuir adsorption theory,  $\theta_j$  is calculated as follows

$$\theta_j = \frac{C_j f_j}{1 + \sum_k C_k f_k} \quad (9)$$

The Langmuir constant  $C_j$  is formulated as

$$C_j = X_j \exp\left(\frac{Y_j}{T - Z_j}\right) \quad (10)$$

The constants  $A_i'$ ,  $B_i'$ , and  $C_i'$  in eq 8 and the constants  $X_i$ ,  $Y_i$ , and  $Z_i$  in eq 10 are listed in Table 1. The binary interaction coefficient between  $\text{CH}_4$  and THF,  $A_{ij}$ , in eq 8 is equal to 165.25.

It could be seen from eq 5 that the filling of small cavities by small size gas molecules could increase driving force. A typical example is the hydrate formed from the ( $\text{CH}_4 + \text{C}_3\text{H}_8$ ) gas mixture. When pure propane hydrate is formed, the small cavities are essentially empty. For a ( $\text{CH}_4 + \text{C}_3\text{H}_8$ ) mixture, however, the small cavities around large cavities could be occupied by methane molecules. When methane molecules fill the small cavities, the fugacity of propane required to form a stable structure II hydrate is reduced (compared with that of pure propane).<sup>12</sup> Although the propane content in the gas mixture is very low (e.g., mole fraction < 0.05), it is enough for propane to form a stable structure II hydrate, and propane content in basic hydrate (large cavities) is very high. This implies that the formation of the mixture hydrate is dominated by propane, and methane adsorbed in small cavities plays a role of help gas only.

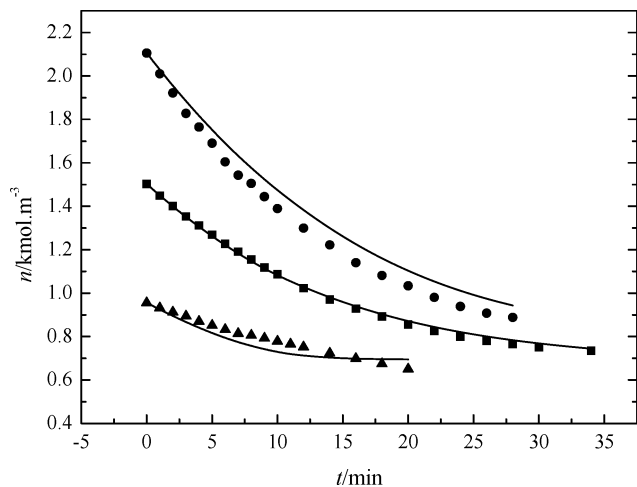
### Results and Discussion

**Experimental Results.** As a kind of selective promoter, THF dissolves in water and forms hydrate easily. The hydrate formation pressure can be lowered enormously with the addition of THF into water.

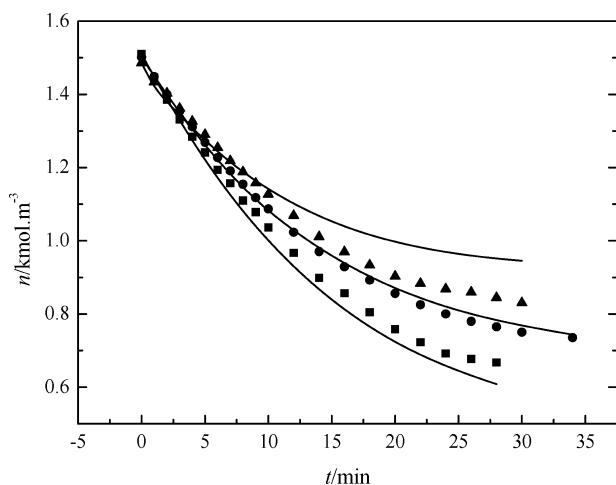
The gas hydrate formation rate for the ( $0.6521\text{CH}_4 + 0.3479\text{C}_2\text{H}_4$ ) gas mixture in the presence of 0.06 mol fraction THF in water was measured by recording the pressure drop at a given temperature in the constant volume batch reactor. To

Table 1. Values of Constants in Hydrate Model (sII)

|                        | $A' \cdot 10^{-22}$ | $B'$     | $C'$   | $X \cdot 10^5$    | $Y$     | $Z$   |
|------------------------|---------------------|----------|--------|-------------------|---------|-------|
| component              | MPa                 | K        | K      | $\text{MPa}^{-1}$ | K       | K     |
| THF                    | 20.5                | -24787.5 | -130.0 | 0                 | 0       | 0     |
| $\text{C}_2\text{H}_4$ | 0.29201             | -13687.5 | 0.6945 | 0                 | 0       | 0     |
| $\text{CH}_4$          | 5.2602              | -12955   | 4.08   | 2.3048            | 2752.29 | 23.01 |



**Figure 2.** Rate of gas consumption for (CH<sub>4</sub> + C<sub>2</sub>H<sub>4</sub>) with mole fraction of 0.06 THF in aqueous solution under different initial pressures. ▲, Experimental data ( $P_0 = 2$  MPa); ■, Experimental data ( $P_0 = 3$  MPa); ●, Experimental data ( $P_0 = 4$  MPa); —, Calculation results.



**Figure 3.** Rate of gas consumption for (CH<sub>4</sub> + C<sub>2</sub>H<sub>4</sub>) with mole fraction of 0.06 THF in aqueous solution under different temperatures. ■, Experimental data ( $T = 273.15$  K); ●, Experimental data ( $T = 274.15$  K); ▲, Experimental data ( $T = 276.15$  K); —, Calculation results.

obtain the mole number of gas in the gas phase, the following equation was used

$$n = \frac{PV}{ZRT} \quad (11)$$

where the compressibility factor  $Z$  was calculated by the Petal–Teja Equation of State (PT EOS).  $V$  is the volume of the gas phase in the reactor. The influences of temperature and initial experimental pressure on the kinetics of hydrate formation were tested, respectively. Figure 2 shows the curves of the amount of gas,  $n$ , in the gas phase over time at a temperature of 274.15 K when different initial pressures  $P_0$  were given. The influences of temperature on gas consumption are plotted in Figure 3 where the initial pressure was 3 MPa. From Figures 2 and 3, it could be seen that the curve slope decreased gradually with time, which means the rate of gas consumption decreased. The reason for this is that the system pressure decreased gradually due to the gas molecules transferred from the gas phase to the hydrate phase during the experiment. The gas compositions in the gas phase over time are listed in Table 2.

**Table 2.** Mole Fraction of Ethylene in the Gas Phase during Hydrate Formation for (CH<sub>4</sub> + C<sub>2</sub>H<sub>4</sub>) with Mole Fraction of 0.06 THF in Water at  $T = 274.15$  K and Different Initial Pressures  $P_0$

| $P_0/\text{MPa} = 2$ |                |                            | $P_0/\text{MPa} = 3$ |                |                            | $P_0/\text{MPa} = 4$ |                |                            |
|----------------------|----------------|----------------------------|----------------------|----------------|----------------------------|----------------------|----------------|----------------------------|
| time/min             | $P/\text{MPa}$ | $y_{\text{C}_2\text{H}_4}$ | time/min             | $P/\text{MPa}$ | $y_{\text{C}_2\text{H}_4}$ | time/min             | $P/\text{MPa}$ | $y_{\text{C}_2\text{H}_4}$ |
| 0                    | 2.0            | 0.3479                     | 0                    | 3.0            | 0.3479                     | 0                    | 4.0            | 0.3479                     |
| 2                    | 1.91           | 0.4040                     | 2                    | 2.81           | 0.3880                     | 2                    | 3.69           | 0.3773                     |
| 4                    | 1.82           | 0.4471                     | 4                    | 2.64           | 0.4155                     | 4                    | 3.42           | 0.3988                     |
| 6                    | 1.74           | 0.4951                     | 6                    | 2.48           | 0.4435                     | 6                    | 3.14           | 0.4219                     |
| 8                    | 1.68           | 0.5484                     | 8                    | 2.34           | 0.4718                     | 8                    | 2.96           | 0.4467                     |
| 10                   | 1.62           | 0.6072                     | 10                   | 2.21           | 0.5003                     | 10                   | 2.75           | 0.4732                     |
| 14                   | 1.50           | 0.7047                     | 14                   | 1.99           | 0.5277                     | 12                   | 2.59           | 0.4872                     |
| 18                   | 1.40           | 0.7741                     | 18                   | 1.84           | 0.5541                     | 14                   | 2.45           | 0.5016                     |
| 25                   | 1.28           | 0.8431                     | 22                   | 1.71           | 0.5795                     | 18                   | 2.19           | 0.5319                     |
| 30                   | 1.20           | 0.8756                     | 26                   | 1.62           | 0.6044                     | 22                   | 2.00           | 0.5640                     |
|                      |                |                            | 34                   | 1.53           | 0.6413                     | 28                   | 1.82           | 0.6156                     |

**Table 3.** Rate of Hydrate Formation from the (CH<sub>4</sub> + C<sub>2</sub>H<sub>4</sub>) Gas Mixture in the Presence of Mole Fraction of 0.06 THF in Water

| $T/\text{K} = 273.15$ |   | $T/\text{K} = 274.15$ |   | $T/\text{K} = 276.15$ |   |
|-----------------------|---|-----------------------|---|-----------------------|---|
| $P$                   | $r$   | $P$                   | $r$   | $P$                   | $r$   |
| MPa                   | $\text{kmol}\cdot\text{m}^{-3}\cdot\text{min}^{-1}$ | MPa                   | $\text{kmol}\cdot\text{m}^{-3}\cdot\text{min}^{-1}$ | MPa                   | $\text{kmol}\cdot\text{m}^{-3}\cdot\text{min}^{-1}$ |
| 3.0                   | 0.05707   | 3.0                   | 0.05248   | 3.0                   | 0.04479   |
| 2.88                  | 0.0549  | 2.9                   | 0.05014   | 2.9                   | 0.04307   |
| 2.77                  | 0.05276   | 2.81                  | 0.04785   | 2.84                  | 0.04136   |
| 2.67                  | 0.05065   | 2.72                  | 0.04561   | 2.76                  | 0.03968   |
| 2.58                  | 0.04856   | 2.64                  | 0.04343   | 2.69                  | 0.03803   |
| 2.5                   | 0.0465  | 2.56                  | 0.0413  | 2.62                  | 0.03639   |
| 2.41                  | 0.04446   | 2.48                  | 0.03922   | 2.55                  | 0.03477   |
| 2.34                  | 0.04245   | 2.41                  | 0.0372  | 2.48                  | 0.03317   |
| 2.25                  | 0.04047   | 2.34                  | 0.03523   | 2.42                  | 0.0316  |
| 2.19                  | 0.03851   | 2.27                  | 0.03332   | 2.36                  | 0.03004   |
| 2.11                  | 0.03658   | 2.21                  | 0.03146   | 2.3                   | 0.02851   |
| 1.98                  | 0.03279   | 2.09                  | 0.0279  | 2.19                  | 0.02551   |
| 1.85                  | 0.0291  | 1.99                  | 0.02456   | 2.08                  | 0.02259   |
| 1.77                  | 0.02552   | 1.91                  | 0.02144   | 2.00                  | 0.01976   |
| 1.67                  | 0.02204   | 1.84                  | 0.01853   | 1.93                  | 0.01701   |
| 1.58                  | 0.01866   | 1.77                  | 0.01583   | 1.87                  | 0.01434   |
| 1.51                  | 0.01538   | 1.71                  | 0.01336   | 1.83                  | 0.01176   |
| 1.45                  | 0.01221   | 1.66                  | 0.01109   | 1.8                   | 0.00927   |
| 1.42                  | 0.00914   | 1.62                  | 0.00905   | 1.78                  | 0.00686   |
| 1.4                   | 0.00617   | 1.59                  | 0.00722   | 1.75                  | 0.00453   |
|                       |   | 1.56                  | 0.0056  |                       |   |
|                       |   | 1.53                  | 0.00302   |                       |   |

It could be seen that the mole fraction of C<sub>2</sub>H<sub>4</sub> was enriched in the gas phase due to the fact that THF can occupy large cavities in the hydrate more easily than ethylene and ethylene molecules could hardly occupy small cavities. The occupancy of small cavities is dominated by methane molecules. Consequently, the occupancy of ethylene molecules in hydrate is inhibited. The difference of gas composition in the gas phase and the hydrate phase indicates the feasibility of separating the gas mixture by forming gas hydrate. The mole fraction of ethylene in the gas phase was enriched from 0.3479 to 0.8756 when initial pressure was at 2 MPa, whereas it was enriched to around 60 % when the initial pressure was at 4 MPa. The amount of gas in the batch reactor was less at low pressure than that at high pressure; therefore, the change of composition in the gas phase was greater at the former conditions. The rates of hydrate formation are given in Table 3. The experimental data show that the initial pressure and system temperature have great influences on the kinetics of hydrate formation. High initial pressure and low temperature could accelerate gas hydrate formation because they provide a larger driving force.

**Calculating Results.** In this work, we used PT EOS to calculate the fugacity of gas species. The experimental data of pure gas by Englezos et al.<sup>4</sup> were used to determine the parameters of hydrate formation kinetics in eq 4 for methane which are listed in Table 4. The correlation results of the gas consumption rate for methane are plotted in Figure 4. On the

**Table 4. Parameters in Equation 4**

| system                        | K   |                  |     | data source |
|-------------------------------|---|------------------|-----|-------------|
|                               | $\text{kmol}\cdot\text{m}^{-3}\cdot\text{min}^{-1}$ | $A\cdot 10^{-7}$ | $n$ |             |
| CH <sub>4</sub>               | 0.090204  | -0.0252454       | 1   | 4           |
| C <sub>2</sub> H <sub>4</sub> | 0.742537  | 27.4787008       | 1   | thiswork    |
| THF                           | 0.014262  | 3.7424927        | 0.5 | 9           |

basis of the Chen–Guo two-step hydrate formation mechanism, the second step (the adsorption of gas molecules into the empty small cavities) could progress much faster than the first step (the formation of a stoichiometric basic hydrate). That means that formation of basic hydrate is the control step during the procedure of whole hydrate formation. The parameters in eq 4 for the mixture were determined by following the mixing rules

$$K = \sum_i x_i^* K_i \quad (12)$$

$$A = \sum_i x_i^* A_i \quad (13)$$

where  $x_i^*$  denotes the mole fraction of gas component  $i$  in basic hydrate. Constant  $n$  was taken to be 1 for pure gas and 0.5 for the gas mixture with THF.

The comparisons of predicted and experimental data of gas mole number in the vapor phase for the (CH<sub>4</sub> + C<sub>2</sub>H<sub>4</sub> + THF) system are presented in Figures 2 and 3. The comparisons of calculated hydrate formation rate with experimental data are presented in Figure 5. It could be seen that the calculating results are in good accordance with experimental data. The proposed algorithm of hydrate formation kinetics provides a valuable tool for simulating and designing the industrial process of separating a gas mixture through forming gas hydrate. The generalized model could predict the kinetics of hydrate formation from gas mixtures as long as the individual parameters have been determined.

In addition, the effect of gas composition in hydrate on driving force was examined. Figure 6 compares the driving force versus pressure using two calculation methods for hydrate from pure methane at 275 K and the formation of sI type hydrate and Figure 7 for the (CH<sub>4</sub> + C<sub>2</sub>H<sub>4</sub> + THF) system. One method assumed that the fractional filling of cavities with gas in hydrate stayed constant which was determined by the three-phase equilibrium pressure at a given temperature, and the other

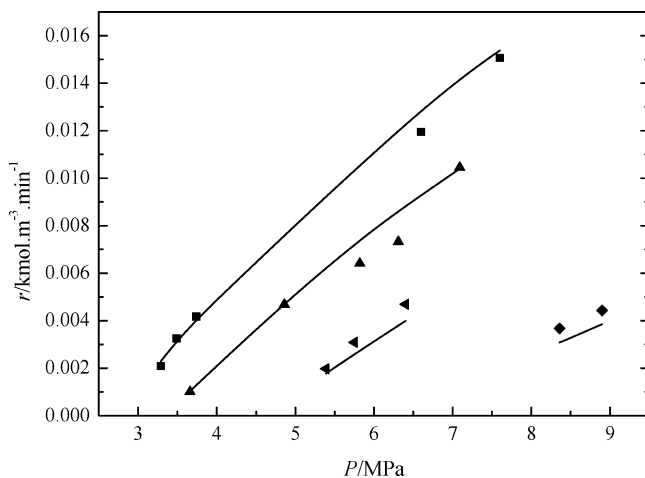


**Figure 4.** Comparison of calculated hydrate formation rate with experimental data<sup>4</sup> for methane. ■, Experimental data ( $T = 274$  K); ▲, Experimental data ( $T = 276$  K); Solid triangle pointing left, Experimental data ( $T = 279$  K); ◆, Experimental data ( $T = 282$  K); —, Calculation results.

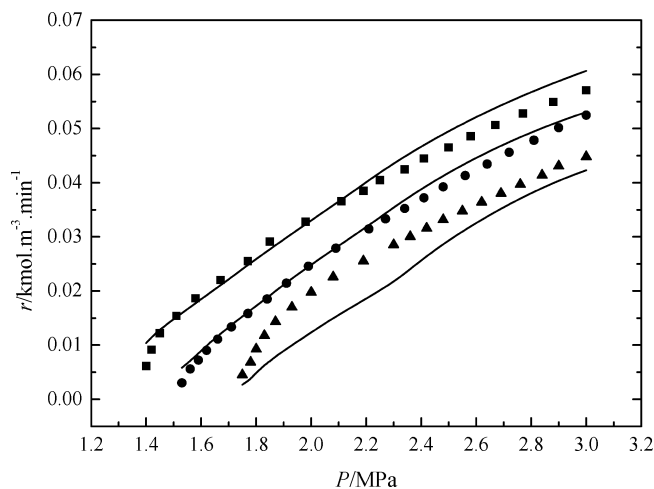


**Figure 5.** Comparison of predicted hydrate formation rate with experimental data for (0.6389CH<sub>4</sub> + 0.3611C<sub>2</sub>H<sub>4</sub>) in 0.06 mol fraction THF aqueous solution. ■, Experimental data ( $T = 273.15$  K); ●, Experimental data ( $T = 274.15$  K); ▲, Experimental data ( $T = 276.15$  K); —, Calculation results.

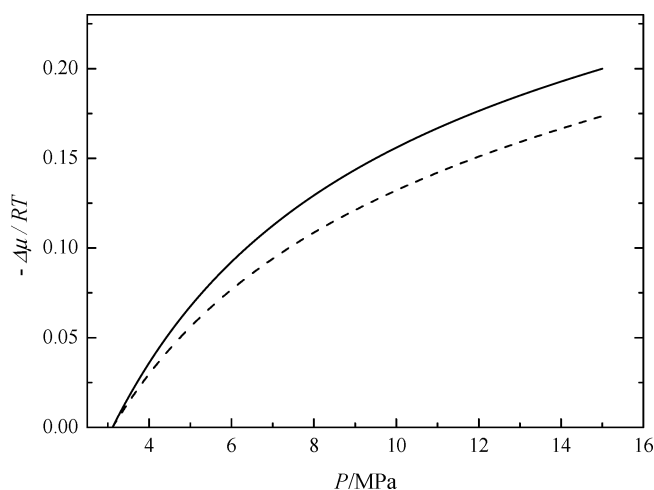


**Figure 6.** Comparison of driving forces using two calculation methods for pure methane at 275 K (sI hydrate). —, Fractional filling of cavities changed; ----, Fractional filling of cavities was constant.

assumed that the fractional filling of small cavities changed with pressure (due to the fractional filling of large cavities being 100 % based on the Chen–Guo model). The result is similar to what Anklam and Firoozabadi<sup>13</sup> obtained. The difference in driving force using the two calculation methods for pure methane is much smaller than that for the (CH<sub>4</sub> + C<sub>2</sub>H<sub>4</sub> + THF) system since the methane filling of cavities for pure methane increases with pressure more slightly than that for the multi-component system.

## Conclusion

Experimental data on the kinetics of gas hydrate formation from a (CH<sub>4</sub> + C<sub>2</sub>H<sub>4</sub>) gas mixture in the presence of THF in water were presented. The experimental results demonstrated that the rate of gas hydrate formation is larger at high pressure and low temperature. The obtained experimental data are valuable for designing the industrial process of separating ethylene-containing gas mixtures by forming hydrates. The kinetic model by Firoozabadi et al. was extended to describe the kinetics of gas hydrate formation from mixtures with THF

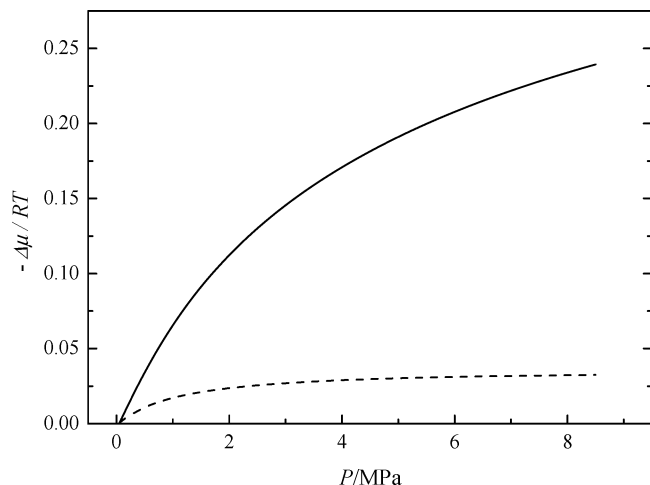


**Figure 7.** Comparison of driving forces using two calculation methods for  $(0.6389\text{CH}_4 + 0.3611\text{C}_2\text{H}_6)$  in 0.06 mol fraction aqueous solution at  $T = 275\text{ K}$ . —, Fractional filling of cavities changed; ----, Fractional filling of cavities was constant.

in water. The difference between the chemical potential of a hydrate building unit in the aqueous solution and in the hydrate crystal was used as the driving force, which was calculated by the Chen–Guo hydrate model. The composition in the hydrate was taken to be a function of pressure which gives rise to high calculation precision of driving force especially for the multi-component system. The parameters for mixtures in the kinetic model were calculated directly from those of pure components. The algorithm is found to describe the experimental data very well.

## Literature Cited

- (1) Sloan, E. D. *Clathrate hydrates of natural gases*, 2nd ed.; Marce Dekker: New York, 1998.
- (2) Vysniauskas, A.; Bishnoi, P. R. A Kinetic Study of Methane Hydrate Formation. *Chem. Eng. Sci.* **1983**, *38*, 1061–1072.
- (3) Vysniauskas, A.; Bishnoi, P. R. Kinetics of ethane hydrate formation. *Chem. Eng. Sci.* **1985**, *40*, 299–303.
- (4) Englezos, P.; Kalogerakis, N.; Dholabhai, P. D.; Bishnoi, P. R. Kinetics of formation of methane and ethane gas hydrates. *Chem. Eng. Sci.* **1987**, *42*, 2647–2658.
- (5) Englezos, P.; Kalogerakis, N.; Dholabhai, P. D.; Bishnoi, P. R. Kinetics of gas hydrates formation from mixtures of methane and ethane. *Chem. Eng. Sci.* **1987**, *42*, 2659–2666.
- (6) Kashichiev, D.; Firoozabadi, A. Nucleation of gas hydrates. *J. Cryst. Growth* **2002**, *243*, 476–489.
- (7) Kashichiev, D.; Firoozabadi, A. Induction time in crystallization of gas hydrates. *J. Cryst. Growth* **2003**, *250*, 499–515.
- (8) Kashichiev, D.; Firoozabadi, A. Driving force for crystallization of gas hydrates. *J. Cryst. Growth* **2002**, *241*, 220–230.
- (9) Duarte, A. R.; Peters, C.; Zevenbergen, J. Kinetics of formation and dissociation of sII hydrogen clathrate hydrates. *Proceedings of the 6th International Conference on Gas Hydrates*, Vancouver, British Columbia, CANADA, July 6–10, 2008.
- (10) Chen, G. J.; Guo, T. M. A new approach to gas hydrate modeling. *Chem. Eng. J.* **1998**, *71*, 145–151.
- (11) Wilson, G. M. Vapor-liquid equilibria XI: a new expression for the excess Gibbs energy of mixing. *J. Am. Chem. Soc.* **1964**, *86*, 127–130.
- (12) Thakore, J. L.; Holder, G. D. Solid-vapor azeotropes in hydrate-forming systems. *Ind. Eng. Chem. Res.* **1987**, *26*, 462–469.
- (13) Anklam, M. R.; Firoozabadi, A. Driving force and composition for multicomponent gas hydrate nucleation from supersaturated aqueous solutions. *J. Chem. Phys.* **2004**, *121*, 11867–11875.

Received for review January 6, 2009. Accepted March 18, 2009.

JE900017K